



Dynamic Analysis of Performance of Photovoltaic Generators under Moving Cloud Conditions

Stephen Ndubuisi Nnamchi^{1a*}, Onyinyechi Adanma Nnamchi^b, Oluwatosin Dorcas Sanya^c, Mustafa Muhamad Mundu^d and Vincent Gabriel^c

- Department of Mechanical Engineering, Kampala International University, Ggaba Road, Kansanga, P.O.B 20000 Kampala, Uganda, stephen.nnamchi@kiu.ac.ug, ORCID: 0000-0002-6368-2913.
- Department of Agricultural Engineering and Bio Resources, Michael Okpara University of Agriculture, Umudike, Umuahia, Nigeria, onyxhoni@yahoo.com, ORCID: 0000-0003-4099-601X.
- Department of Electrical/Telecommunication/Computer Engineering, SEAS, Kampala International University (KIU), P.O.B 20000 Ggaba Road, Kansanga, Kampala, Uganda.
- Department of Physical Sciences, SEAS, Kampala International University, P.O. Box 20000, Kampala, Uganda, mundu.mustafa@kiu.ac.ug, ORCID: 0000-0003-1345-9999.

^aFirst affiliation, Address, City and Postcode, Country

^bSecond affiliation, Address, City and Postcode, Country

Received: 15.06.2020

Accepted: 04.08.2020

Abstract

Dynamic analysis of performance of photovoltaic generators (PVG) under moving cloud conditions has been successfully carried out. The research work aims at eliminating under-performance contributed by the manufacturer's specification. The PVG characteristics were simulated in Microsoft Excel environment under simple and superimposed conditions, designating mild and strong cloud conditions, respectively with modified and unmodified PVG parameters. Concurrently, field measurement of the performance characteristics of PVG was carried out at KIU (0.3476°N, 32.5825°E) upon which the façade in the specification was estimated and reduction in output power under the aforementioned conditions were computed. The power reduction becomes colossal during the superimposed condition. Besides, common operational problems like transients in output voltage and power are remarkable. Thus, the under-performance in large PVG could be narrowed by scaling down the manufacturer's rating or applying the correction factor recommended by this work in large PVG design, hence, leaving the design engineers with the moving cloud problems.

Keywords: Dynamics, analysis, performance rating, PVG, simple and superimposed cloud conditions.

1.0 Introduction

Moving clouds pose serious challenge in the operation of photovoltaic generators (PVG), especially when the size of water droplets are large and nuclei (dusts, aerosols) constituents of the cloud abound in the troposphere, it absorbs the bulk

sunlight needed for the generation of charge carriers (electron-hole) in the semiconductor device whereas light droplet of clouds (cirrus) or clouds free atmosphere may not significantly impede the performance of the PVG. Stochastically, the atmosphere could erratically present different clouds

of different droplet sizes. Thus, the operation of PVG is threatened whenever the dark gray, rainy clouds (nimbus) saturate the atmosphere. Unlike dust coverings which has long-term effect on the PV performance, cloud covering has an instantaneous effect on the PV performance causing voltage to flicker [1].

Concurrently, Mustafa, et al. [2] affirms that rapid moving cloud conditions affect the solar power production; however, he did not quantify the amount of power loss due to the moving clouds. Although it is imperative to estimate the reduction in power due to the moving clouds, which is one of the cardinal drivers of this research work.

Subsequently, Suri et al. [3] proposed that in the event of low cloud cover; the integrated output power from a several PV power plants results in smooth and stable power production, but the persistence overcast of clouds engender a low power production in the same plant; and statistically, power production could be above 75% (< 25% power loss) and less than 35% (> 65% power loss) in low and high clouds cover, respectively [3].

Thus, modern-day quantification of the effect of clouds employs the application of satellites; First and Second Generation Meteosat, MFG and MSG (chiefly, global earth radiation budget, GERB), respectively, and Ground Station Measurements (GSM). Both techniques are affected by complex mountainous terrain. The ground techniques function better than satellite on-site, but off-site (> 30 km), the satellite technique is superior to the ground station measurement [4].

Pertinently, Ye et al. [5] submitted that high irradiance (> 900 W/m²) has a much better impact on the performance of PV module than the low irradiance (< 350 W/m²). Ye et al. [5] applied Adnot clear-sky model which served as a reference for comparing the impact of fluctuating irradiance; high transient irradiance affects the module performance more than the low transient one. However, the impact of fluctuating irradiance would have been more evident by basing the reference on the standard test condition (STC), which is an indoor condition that is void of the influence of the moving clouds. Moreover, they affirmed that the presence of intensity of moving cloud is inversely proportional to a clearness index (sky condition); although, the relationship failed at a latitude of 10N [5, 6].

Besides, the magnitude of insolation is severely affected by the weather change, thus, varying cloud conditions engender erratic variation in the insolation and PV power production, which is responsible for the transients in insolation and the

output power; and for grid-connected PV systems, it becomes difficult to maintain maximum power point with incessant weather change ([7-9]). The authors' deployed experimental techniques only in the research technique; simulation of cloud effects was not incorporated in the research, which is the mainstay of the present work. According to Cirjaleanu [10] and Yan and Saha, [11] voltage instability in large PVG is associated to cloud-effect emanating from the fast movement of the clouds, which causes a fluctuation in the output power.

Additionally, large quick fluctuations in insolation results in a condensed and protracted variation in the PV output power. Nevertheless, a cloud-induced change in insolation can alter the operating conditions of a PV system. The parameters altered by changes in insolation; include the PV array's operating DC voltage, and PV plant's power generation capabilities [12].

Assiduously, Cai [13] investigated power transitions and its possible effect on the grid, by deploying Modified Midpoint Displacement Algorithm which supposedly is capable of generating the cumulus cloud with emphasis on; the thickness, velocity, time-series, which is capable of simulating the measured irradiance at any location. However, the simulated data were not compared with the practical values to ascertain the fitness between the simulated and measured results. Cai [13] and Marcos et al. [14] proposed that the distributed insolation gave better results than the lumped one of thousands of PV modules spread over a wide area. These works did not draw out the influence of irradiance on the output power; but the present work intends to show pictorially and numerically the influence of insolation on the measured and simulated output current, voltage and power transitions.

Alternatively, Osma et al. [15] deployed the Degree of Freedom (DOF) techniques in the analysis of the influence of the moving cloud on the PV transients, the technique considers the full cloud shadow on the PV module known as the upper limit and partial covering of the cloud shadow on the PV module known as the lower limit. The method further compensates the upper limit with arbitrary power (+3 W) whereas deprive the lower limit by the same amount of power (-3W); such that the average parameters obtained from both upper and lower limits are in close tie. Supposedly, the compensated power represents the drop in power. Furthermore, they introduced a normalized voltage and current curves which serve as a means of detecting faults in a PVG system. However, the

present work will estimate drops in parameters by considering the difference in the parameters at STC and actual operating conditions (AOC). The present work intends to display a dynamic current and voltage curves to reflect the fluctuations in insolation.

Cautiously, Bellini et al. [16] stated that the majority of literature on the dynamic simulation of the performance of the PV modules, ignored the influence of insolation on the voltage, truly, voltage is independent of insolation. They proposed that the open circuit and maximum power voltages as a dual function of the PV-cell temperature and insolation; the pitfall of the technique is that all the performance parameters were specified to avoid the application of numerical scheme in solving the non-linear equivalent circuit model deployed in the performance analysis of the PV systems. The present work holds a similar modification by creating PV-cell temperature as a function of insolation through a thermal balance [17], and open circuit voltage as a function of the PV-cell temperature; thus, the open circuit voltage is formulated as a function of insolation in order to reflect the influence of insolation change on the voltage.

Essentially, Esmeijer [18] propounded that precipitation induces a blue shift in the solar spectrum, which increases the short-circuit current of the modules (particularly for a-Si and CdTe), and causes module temperature to drop, thus resulting in an increase in open-circuit voltage for all modules. The first proposition could be true to the premise that precipitation has potential to increase the intensity of insolation but the second proposition is universally accepted. According to Abdellatif et al. [7] the insolation transients are responsible for grid instability and penetration rate depending on the size of the power plant. The authors recommended that the application of accessories like inverter in order to control power surge and battery for maintaining stable voltage.

Prominently, the performance specification of solar cell modules by the manufacturers does not accurately reflect the efficiency of the PVG at the time of use because the performance specification at STC is usually done in the absence of clouds. The authors established that variation in irradiance for large PV plants by formulating short circuit current and open circuit voltage, which is space dependent. Thus, the spatial distribution of irradiance caused by the moving cloud could be visualized. The authors did not consider the time variation of the parameters of actual operating conditions (AOC) but the present work will articulate the overall change in parameters

at STC by modifying them and to reflect the dynamism of moving clouds on the PVG output power at AOC [19, 20].

Thus, considering the gaps enumerated in the referenced literature, hence, the present work is geared towards dynamic quantification of reduction or losses in the output power of PVG due to the moving clouds; basically, to unveil the true performance of PVG under actual operating conditions against the standard test condition; and subsequently to propose correction factor which addresses facades in the specification of standard test condition. The rest of the article include; materials and method, result presentation and discussion, conclusions and recommendation.

2. Materials and Methods

An outdoor experimental testing facility in Figure 1 is set up under the climatic conditions of Kansanga, Kampala, Uganda. The facility consists of two Mira Cozy PV modules (MC010W-18P), a deep cycle battery (GOLD STAR 12V/7Ah), 5A solar power charge controller, an inverter (S-300W 230V/50Hz AC 12V DC), a digital multi-meter (DT-9205A), a digital multi-meter (UT33 with UT33C thermocouple) and a light bulb (20W DC). The following data were recorded; air temperature, PV glass temperature, base/tehdar temperature, PV output voltage and current, and load voltage and current. Readings were recorded every 15 minutes from 6:00 GMT to 19:00 GMT. The experiment was conducted for six (6) consecutive time in each month between January to April and the glass and base_tedlar temperature were used to validate the simulated result under moving cloud conditions. In addition a 10 year meteorological data on insolation, air temperature and wind speed for the study location were acquired from meteorological centers [21-23] ranging from 2007 to 2017.



Figure 1. An outdoor experimental testing facility

3.0 PV Electrical Performance Model Formulation

The typical non-linear equivalent circuit model describing the behaviour of photovoltaic generators (PVG) under moving cloud conditions [24] is expressed in Equations 1 as

$$I = \left[I_{ph} - I_0 \left(\exp \left(\frac{V + IR_s}{A V_T} \right) - 1 \right) - \frac{V + IR_s}{R_p} \right] \quad (1)$$

where I (A) is the output current; V (V) is the output voltage; I_{ph} (A) is the photon current; I_0 (A) is the diode saturation or reverse current; A (-) is the ideality factor which is equal to or greater one (≥ 1) for ideal and real equivalent circuit models, respectively [25]; V_T (V) is the thermal voltage; R_s (Ω) is the series resistance; R_p (Ω) is the shunt or parallel resistance and the subscript designates the standard or ambient condition.

3.1 PV Performance Analysis at Standard Test Condition (STC $\equiv 0$)

The PV cell is characterized by three principal indoor conditions; short circuit (SC), maximum power point (MPP) and open circuit (OC).

For SC: $I = I_{sc}$; $V = 0$. Substituting SC conditions into Equation 1 gives Equation 2

$$I_{sc} = I_{ph0} - I_{00} \left(\exp \left(\frac{I_{sc} R_{s0}}{A_0 V_T} \right) - 1 \right) - \frac{I_{sc} R_{s0}}{R_{p0}} \quad (2)$$

For MPP: $I = I_{mpp}$; $V = V_{mpp}$; substituting MPP conditions into Equation 1 gives Equation 3

$$I_{mpp} = I_{ph0} - I_{00} \left(\exp \left(\frac{V_{mpp} + I_{mpp} R_{s0}}{A_0 V_T} \right) - 1 \right) - \frac{V_{mpp} + I_{mpp} R_{s0}}{R_{p0}} \quad (3)$$

For OC: $I = 0$; $V = V_{oc}$; substituting OC conditions into Equation 1 gives Equation 4

$$0 = I_{ph0} - I_{00} \left(\exp \left(\frac{V_{oc}}{A_0 V_T} \right) - 1 \right) - \frac{V_{oc}}{R_{p0}} \quad (4)$$

Combining Equations 2 – 4 algebraically yield Equations 5 – 7 at standard test condition (STC)

The photon current, I_{ph0} (A) at STC in Equation 5 merges as

$$I_{ph0} \Big|_j = \frac{\begin{pmatrix} I_{sc} V_{oc} \left(\exp \left(\frac{V_{mpp} + I_{mpp} R_{s0}}{A_0 V_T} \right) - 1 \right) \\ - I_{sc} V_{oc} \left(\exp \left(\frac{V_{oc}}{A_0 V_T} \right) - 1 \right) \\ - I_{mpp} V_{oc} \left(\exp \left(\frac{I_{sc} R_{s0}}{A_0 V_T} \right) - 1 \right) \end{pmatrix}}{\begin{pmatrix} (V_{oc} - I_{sc} R_{s0}) \left(\exp \left(\frac{V_{mpp} + I_{mpp} R_{s0}}{A_0 V_T} \right) - 1 \right) \\ + (V_{mpp} + I_{mpp} R_{s0} - V_{oc}) \left(\exp \left(\frac{I_{sc} R_{s0}}{A_0 V_T} \right) - 1 \right) \\ + (I_{sc} R_{s0} - V_{mpp} - I_{mpp} R_{s0}) \left(\exp \left(\frac{V_{oc}}{A_0 V_T} \right) - 1 \right) \end{pmatrix}}; \quad (5)$$

$$j = \{\text{unmodified} \equiv \text{STC}\}$$

The diode saturation or reverse current, I_{00} (A) in Equation 6 turn into

$$I_{00} \Big|_j = \frac{V_{oc} (I_{sc} - I_{mpp}) - I_{sc} V_{mpp}}{\begin{pmatrix} (V_{oc} - I_{sc} R_{s0}) \left(\exp \left(\frac{V_{mpp} + I_{mpp} R_{s0}}{A_0 V_T} \right) - 1 \right) \\ + (V_{mpp} + I_{mpp} R_{s0} - V_{oc}) \left(\exp \left(\frac{I_{sc} R_{s0}}{A_0 V_T} \right) - 1 \right) \\ + (I_{sc} R_{s0} - V_{mpp} - I_{mpp} R_{s0}) \left(\exp \left(\frac{V_{oc}}{A_0 V_T} \right) - 1 \right) \end{pmatrix}}; \quad (6)$$

$$j = \{\text{unmodified} \equiv \text{STC}\}$$

The shunt resistance, R_{p0} (Ω) at STC, Equation 7 turn out to be

$$R_{p0} \Big|_j = \frac{\begin{pmatrix} (V_{oc} - I_{sc} R_{s0}) \left(\exp \left(\frac{V_{mpp} + I_{mpp} R_{s0}}{A_0 V_T} \right) - 1 \right) \\ + (V_{mpp} + I_{mpp} R_{s0} - V_{oc}) \left(\exp \left(\frac{I_{sc} R_{s0}}{A_0 V_T} \right) - 1 \right) \\ + (I_{sc} R_{s0} - V_{mpp} - I_{mpp} R_{s0}) \left(\exp \left(\frac{V_{oc}}{A_0 V_T} \right) - 1 \right) \end{pmatrix}}{\begin{pmatrix} I_{sc} \left(\exp \left(\frac{V_{mpp} + I_{mpp} R_{s0}}{A_0 V_T} \right) - 1 \right) \\ - I_{mpp} \left(\exp \left(\frac{I_{sc} R_{s0}}{A_0 V_T} \right) - 1 \right) \\ + (I_{mpp} - I_{sc}) \left(\exp \left(\frac{V_{oc}}{A_0 V_T} \right) - 1 \right) \end{pmatrix}}; \quad (7)$$

$$j = \{\text{unmodified} \equiv \text{STC}\}$$

Ideality factor, A (-) in Equation 8 is expressed in [26] as

$$A = \frac{I_{mpp} V_{oc}}{I_{sc} V_{mpp}} \quad (8)$$

The thermal voltage, V_T (V) in Equation 9 is defined in [27] as

$$V_T = \frac{n_s K_B T_{pv}}{q_c} \quad (9)$$

where n_s (-) is the total number of series cells in a module.

The series resistance, R_s (Ω) in Equation 10 is expressed in [26] as

$$R_s = \frac{n_p}{n_s} \left(1 - \frac{I_{mpp} V_{mpp}}{I_{sc} V_{oc}} \right) \left(\frac{V_{oc}}{I_{sc}} - \frac{V_{mpp}}{I_{mpp}} \right) \quad (10)$$

where n_p (-) is the total number of parallel cells in a module.

3.2 Parameter Modification: Short circuit Current and Open Circuit Voltage

Modification of STC is centered on the short circuit current, I_{sc} and the open circuit voltage, V_{oc} , respectively in Equation 11 as follows [28]:

$$I'_{sc} = I_{sc} + k_t \Delta T ; V'_{oc} = V_{oc} + k_v \Delta T ; \quad (11)$$

$$\Delta T = T_{pv} - T_a$$

Substituting Equation 11 into Equations 5 – 7 gives Equations 12 – 14.

The modified photon current, I_{ph0} (A) in Equation 12 is expressed as

$$I'_{ph0}|_j = \frac{\left(\begin{array}{l} I'_{sc} V'_{oc} \left(\exp\left(\frac{V_{mpp} + I_{mpp} R'_{s0}}{A'_0 V_T}\right) - 1 \right) \\ - I'_{sc} V'_{oc} \left(\exp\left(\frac{V'_{oc}}{A'_0 V_T}\right) - 1 \right) \\ - I_{mpp} V'_{oc} \left(\exp\left(\frac{I'_{sc} R'_{s0}}{A'_0 V_T}\right) - 1 \right) \end{array} \right)}{\left(\begin{array}{l} (V'_{oc} - I'_{sc} R'_{s0}) \left(\exp\left(\frac{V_{mpp} + I_{mpp} R'_{s0}}{A_0 V_T}\right) - 1 \right) \\ + (V_{mpp} + I_{mpp} R'_{s0} - V_{oc}) \left(\exp\left(\frac{I'_{sc} R'_{s0}}{A'_0 V_T}\right) - 1 \right) \\ + (I'_{sc} R'_{s0} - V_{mpp} - I_{mpp} R'_{s0}) \left(\exp\left(\frac{V'_{oc}}{A'_0 V_T}\right) - 1 \right) \end{array} \right)} ; \quad (12)$$

$$j = \{\text{modified}\}$$

The modified diode saturation or reverse current, I'_{00} (A) in Equation 13 is defined as

$$I'_{00}|_j = \frac{V'_{oc} (I'_{sc} - I_{mpp}) - I'_{sc} V_{mpp}}{\left(\begin{array}{l} (V'_{oc} - I'_{sc} R'_{s0}) \left(\exp\left(\frac{V_{mpp} + I_{mpp} R'_{s0}}{A'_0 V_T}\right) - 1 \right) \\ + (V_{mpp} + I_{mpp} R'_{s0} - V'_{oc}) \left(\exp\left(\frac{I'_{sc} R'_{s0}}{A'_0 V_T}\right) - 1 \right) \\ + (I'_{sc} R'_{s0} - V_{mpp} - I_{mpp} R'_{s0}) \left(\exp\left(\frac{V'_{oc}}{A'_0 V_T}\right) - 1 \right) \end{array} \right)} ; \quad (13)$$

$$j = \{\text{modified}\}$$

The modified shunt resistance, R_{po} (Ω) in Equation 14 is written as

(14) The modified ideality factor, A' (-) in Equation 15 is expressed in as

$$A' = \frac{I_{mpp} V'_{oc}}{I'_{sc} V_{mpp}} \quad (15)$$

The modified series resistance, R'_s (Ω) in Equation 16 is expressed in as

$$R'_s = \left(1 - \frac{I_{mpp} V_{mpp}}{I'_{sc} V'_{oc}} \right) \left(\frac{V'_{oc}}{I'_{sc}} - \frac{V_{mpp}}{I_{mpp}} \right) \quad (16)$$

3.3 PV Performance Analysis of Actual Operating Condition (AOC)

The performance analysis at AOC or outdoor condition is as follows:

$$I_{ph,k}|_j = \frac{G_{T,k}}{G_0} (I_{ph0} + K_t \Delta T) = \frac{G_{T,k}}{G_0} (I_{ph0} + K_t (T_{pv} - T_a))$$

$$j = \{\text{modified, unmodified}\}; \quad (17)$$

$$k = \{\text{simple, superimposed}\}$$

where G_T (W/m^2) and G_0 (W/m^2) is insolation on an inclined surface and at standard test condition (0), K_t ($\%/K$) is current coefficient, T (K) is temperature; the subscripts: pv and a ($\equiv 0$) designate photovoltaic and ambient, respectively.

The diode current, I_0 (A) in Equation 18 is defined in [29] as

$$I_{0,k}|_j = I_{00} \left(\frac{T_a}{T_{pv,k}} \right)^3 \exp\left(\frac{q_c E_g}{A K_B} \left(\frac{1}{T_a} - \frac{1}{T_{pv,k}} \right) \right)$$

$$j = \{\text{modified, unmodified}\}$$

$$k = \{\text{simple, superimposed}\}$$

where I_{00} (A) is the diode reverse or saturation current, q_c (C) is the quantity of electron charge, E_g (eV) is the energy gap of the semiconductor, K_B (J/K) is the Boltzmann constant.

The series resistance, R_s (Ω) in Equation 19 is less susceptible to temperature rise [30] thus

$$R_s|_j \approx R_{s0}$$

$$j = \{\text{modified, unmodified}\}; \quad (19)$$

$$k = \{\text{simple, superimposed}\}$$

The shunt or parallel resistance, R_p (Ω) in Equation 20 is more susceptible to temperature rise, forthwith

$$R_{p,k}|_j = R_{p0} (1 + \beta \Delta T) = R_{p0} (1 + \beta (T_{pv,k} - T_a));$$

$$\beta \approx 2 / (T_{pv,max} + T_a) \quad (20)$$

$$j = \{\text{modified, unmodified}\};$$

$$k = \{\text{simple, superimposed}\}$$

where β (1/K) is a linear temperature coefficient and the subscript max refers to maximum condition.

The output current, I (A) in Equation 21 is computed for $0 < V < Voc$ using Newton-Raphson scheme [31]

$$I_{i+1,k}|_j = I_i - g(I) / g'(I);$$

$$j = \{\text{modified, unmodified}\}; \quad (21)$$

$$k = \{\text{simple, superimposed}\}$$

where $g(I)$ in Equation 22 is a mathematical function of Equation 1

$$g_k(I)_j = I_{ph} - I_0 \left(\exp \frac{V + IR_s}{AV_T} - 1 \right) - \frac{V + IR_s}{R_p} - I = 0 ;$$

$$j = \{\text{modified, unmodified}\}; \quad (22)$$

$$k = \{\text{simple, superimposed}\}$$

whereas $g'(I)$ in Equation 23 is the partial derivative of $g(I)$ with respect to (wrt) current, $I(A)$

$$g'_k(I)_j = -\frac{I_0 R_s}{AV_T} \left(\exp \frac{V + IR_s}{AV_T} \right) - \frac{R_s}{R_p} - 1 = 0$$

$$;$$

$$j = \{\text{modified, unmodified}\};$$

$$k = \{\text{simple, superimposed}\}$$

The output power, $P(W)$ in Equation 24 is given as

$$P_k|_j = IV ;$$

$$j = \{\text{modified, unmodified}\}; \quad (24)$$

$$k = \{\text{simple, superimposed}\}$$

whereas the normalized change in power, $-\Delta P/P(-)$ in Equation 25 is expressed as

$$-\frac{\Delta P(t)}{P_{Theoretical_STC}} \Big|_j = \frac{P_{Actual_simple}(t)}{P_{Theoretical_STC}} - 1$$

or

$$-\frac{\Delta P(t)}{P_{Theoretical_STC}} \Big|_j = \frac{P_{Actual_superimposed}(t)}{P_{Theoretical_STC}} - 1 \quad (25)$$

$$j = \{\text{modified, unmodified}\};$$

$$k = \{\text{simple, superimposed}\}$$

where $t(s)$ is time with 6:00am as a reference time. The maximum efficiency, $\eta_{max}(-)$ of the PVG [32] is defined in Equation 26 as

$$\eta_{max,k}|_j = \frac{I_{mpp} V_{mpp}}{G a} ;$$

$$j = \{\text{modified, unmodified}\}; \quad (26)$$

$$k = \{\text{simple, superimposed}\}$$

where a is the surface area of the PVG available to the insolation.

Obviously due to façade by the manufacturer of PVG, the practical or field efficiency of the PVG are usually less than the manufacturer's rating [33]. Thus, Equation 27 represents constraint between the manufacturer and field rating of PVG as follows:

$$\eta_{max,k}|_{j, manufacturer} > \eta_{max,k}|_{j, field} ; \quad (27)$$

$$j = \text{modified}; k = \text{simple}$$

The correction factor, $cf(%)$ is introduced in Equation 28 to remove the inequality as follows:

$$\eta_{max, manufacturer} = \eta_{max,k}|_{j, field} + cf ; \quad (28)$$

$$j = \text{modified}; k = \text{simple}$$

where $cf(%)$ in Equation 29 is defined as

$$cf = \sqrt{\frac{\sum_{i=1}^n \left(\eta_{max, manufacturer} - \eta_{max,k}|_{j, field} \right)_i^2}{n}} ; \quad (29)$$

$$j = \text{modified}; k = \text{simple}$$

where n is the number of data observed.

According to Topic et al. [33] the performance ratio, $PR(-)$ in Equation 30 is defined as

$$PR_j = \frac{\eta_j}{\eta_{manufacturer(STC)}} ; \quad (29)$$

$$j = \{\text{measured, simulated}\}$$

4.0 Results and Discussion

4.1 Results

The dynamic thermal input data [34] is shown in Figures 2 and 3; depicting the dynamic insolation and PV-cell temperature, respectively for the simple and superimposed cloud conditions. The dynamic insolation model under the influence of the clouds is a function of the amplitude of the solar irradiance, the frequency of weather change, the clearness index which depicts the movement of the clouds and the solar time. The detailed model development is given in Nnamchi et al. [17]. Pertinently, the computation of the PVG parameters is governed by the dynamic thermal input data. Thus, Table 1 presents the electrical parameters used in the simulation of the PVG system (Cozy Mira $\times 2$).

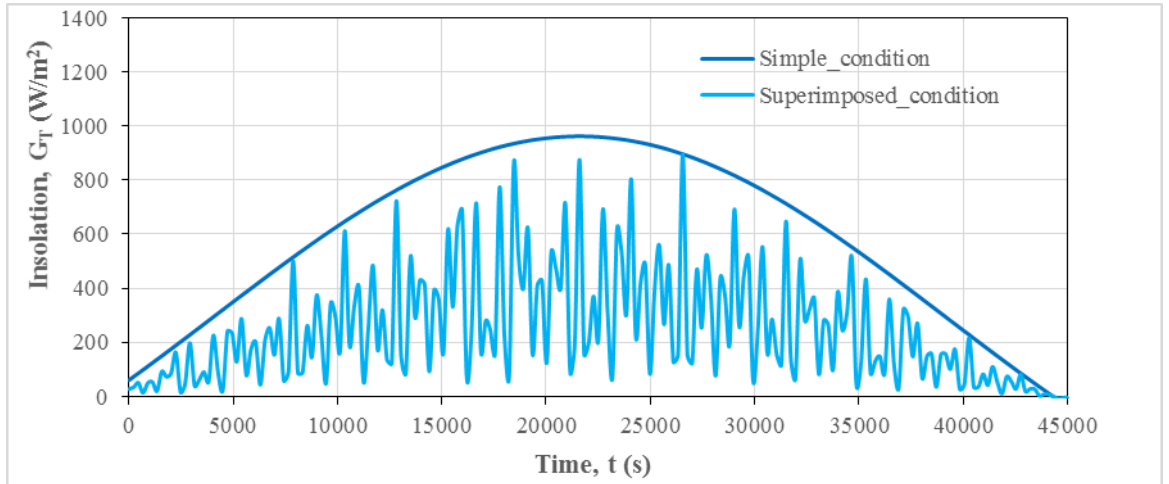


Figure 2. Simulated dynamic insolation input data for latitude, $\phi = 0.3476^\circ\text{N}$, slope, $\varphi=19.5^\circ$, month = January with 6:00am as a reference point.

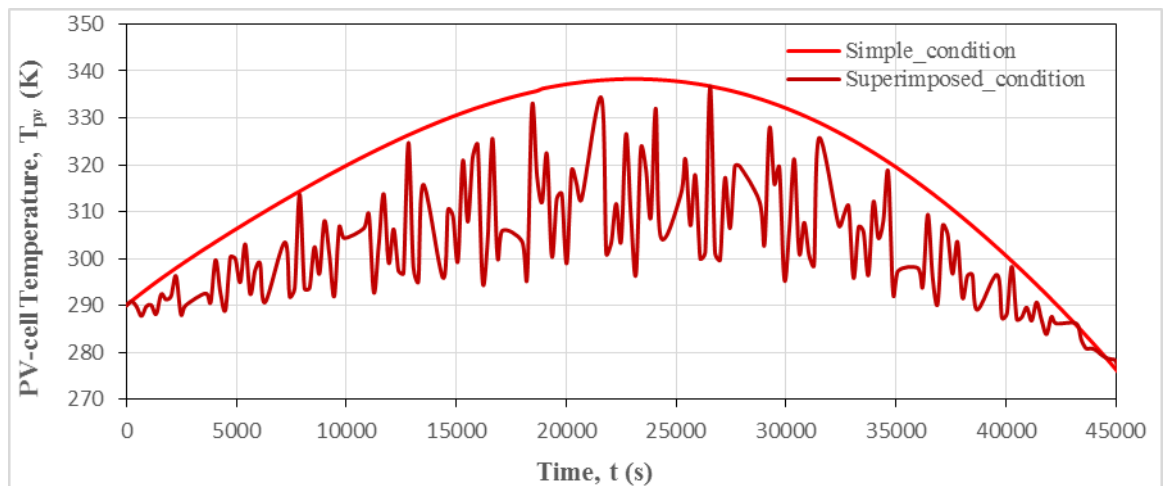


Figure 3. Simulated dynamic PV-cell temperature input data for latitude, $\phi = 0.3476^\circ\text{N}$, slope, $\varphi=19.5^\circ$, month = January with 6.00AM as a reference time.

Table 1. Data for two Mira Cozy modules in the series at AM=1.5 and G=1000 (W/m²)

S/no	Constant /variable	Symbol	Unit	Value
1.	Module type (polycrystalline silicon)	-	-	-
2.	Number of cells in series	n_s	-	36×2
3.	Number of cells in parallel	n_p	-	1
4.	Short circuit current at standard test condition	I_{sc}	A	0.65
5.	Open circuit voltage at standard test condition	V_{oc}	V	21.6×2
6.	Current at maximum power point	I_{mpp}	A	0.58

7.	Voltage at maximum power point	V_{mpp}	V	17.2×2
8.	Temperature coefficient of short circuit current	k_i	%/K	0.065
9.	Temperature coefficient of open circuit voltage	k_v	%mV/K	-80
10.	Temperature at standard test condition	T_0	K	298.15
11.	Irradiance at standard test condition	G_0	W/m ²	1000
12.	Boltzmann constant	K_B	J/K	1.3806×10 ⁻²³
13.	Electron charge	q_e	C	1.6×10 ⁻¹⁹
14.	Energy gap for c-Si (polycrystalline silicon)	E_g	eV	1.11
15.	Ideality factor at standard test condition	A_0	-	1.1206
16.	Parallel resistance at standard test condition (minimum)	$R_{p0,min}$	Ω	557.6755
17.	Series resistance at standard test condition (minimum)	R_{s0}	Ω	0.02875
18.	Diode saturation or reverse current	I_{00}	A	5.2358×10 ⁻¹⁰
19.	Photon or light current	I_{ph0}	A	0.650034

4.2 Discussion

Figures 4 and 5 present the PVG output power as a function of output voltage and time for the simple cloud condition, which portrays mild moving cloud conditions; Figure 4 displays the output power for the unmodified short circuit (SC) current and open circuit (OC) voltage whereas Figure 5 shows that the modified SC (SC') and modified OC (OC'). Figure 4 shows false voltage beyond the manufacturer's

rating because the OC voltage and SC current are insensitive to variations in PV-cell temperature. Contrarily, the output voltage in Figure 5 is below the manufacturer's stipulated voltage because the OC' voltage and SC' current are sensitive to variation in PV-cell temperature. Thus, Figure 5 depicts the true field performance of the PVG under study

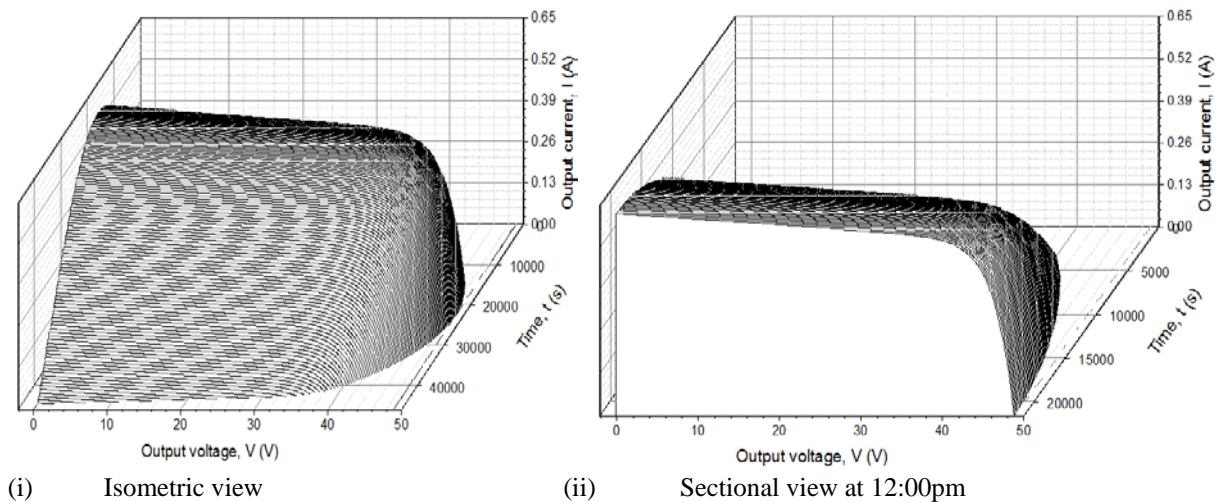


Figure 4a. Unmodified simple current-voltage curves for latitude, $\phi = 0.3476^\circ\text{N}$, slope, $\varphi=19.5^\circ$, month=January with 6:00am as a reference time.

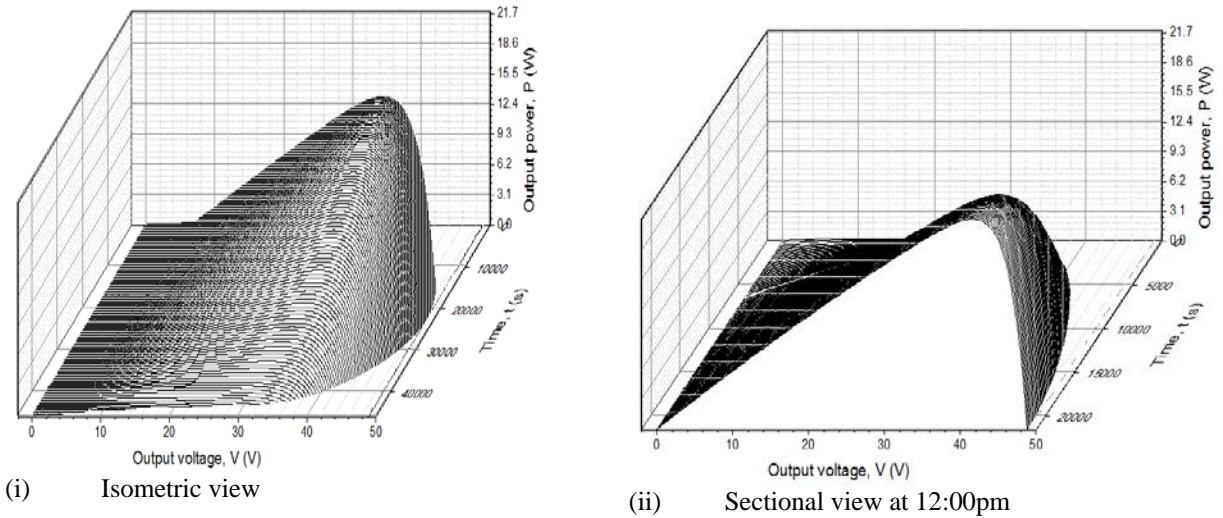


Figure 4b. Unmodified simple power-voltage curves for latitude, $\phi = 0.3476^\circ\text{N}$, slope, $\varphi=19.5^\circ$, month = January with 6:00am as a reference time.

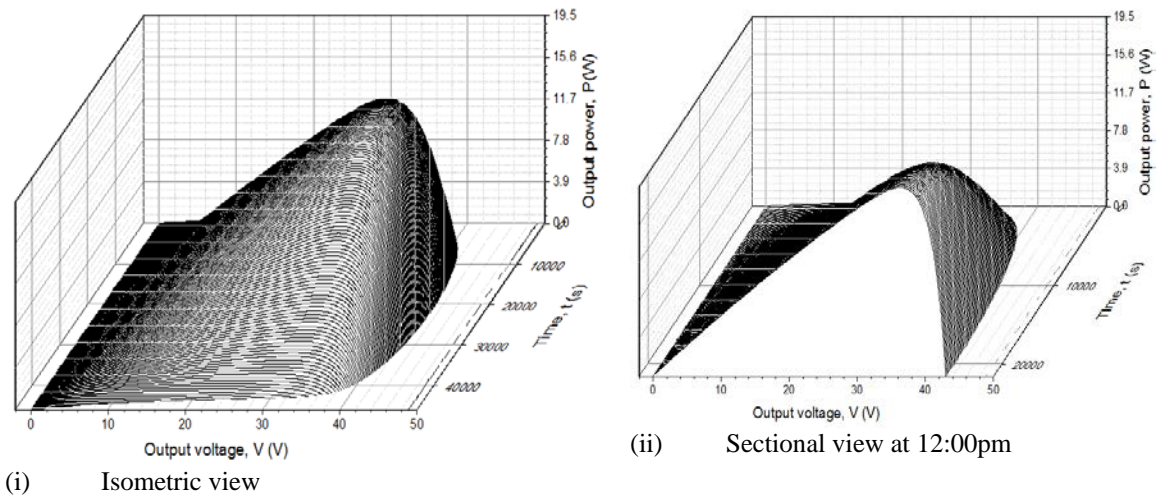


Figure 5b. Modified simple power-voltage curves for latitude, $\phi = 0.3476^\circ\text{N}$, slope, $\varphi=19.5^\circ$, month = January with 6:00am as a reference time.

Figures 6 and 7 illustrate the PVG output power as a function of output voltage and time for superimposed condition, which demonstrates strong moving cloud condition; the phenomenon of pseudo-voltage (Figure 6) and practical voltage (Figure 7) is similar to those of simple condition.

The contrast between Figures (4 and 5) and Figures (6 and 7) is that power harvest abounds in Figures 4 and 5 due to mild cloud conditions [3] but power

harvest in Figures 5 and 6 is sparse due to the strong overcast of moving clouds [2]. Poor power harvest during the superimposed condition is vivid in the detailed view of power in Figures 6ba (ii) and 7b (ii), which are characterized by skeletal power generation relative to their counterparts in Figures 4 and 5.

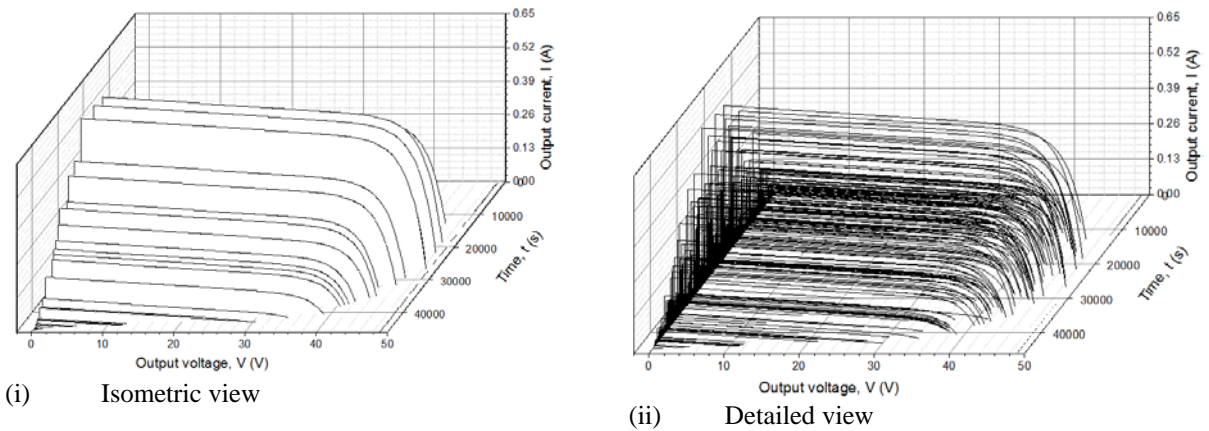


Figure 6a. Unmodified superimposed current-voltage curves for latitude, $\phi = 0.3476^\circ\text{N}$, slope, $\varphi=19.5^\circ$, month = January with 6:00am as a reference time

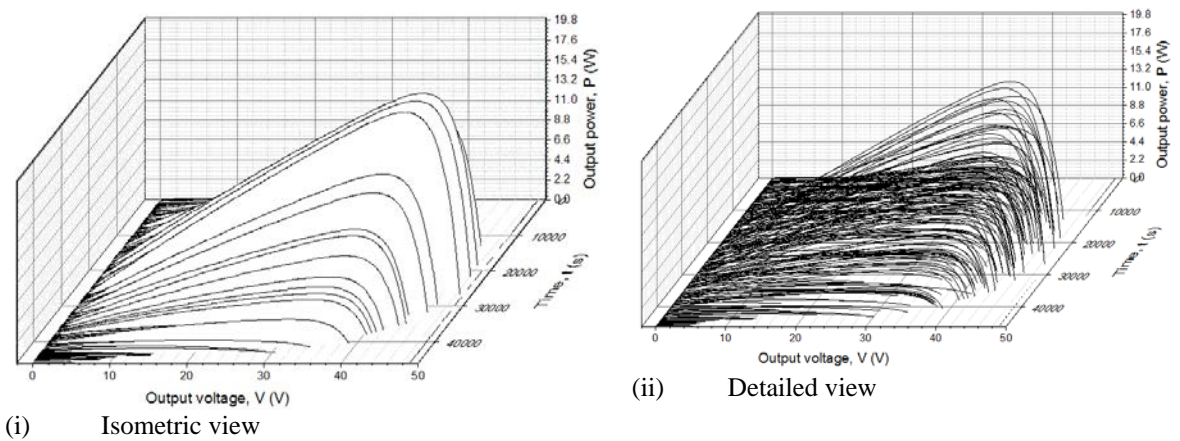
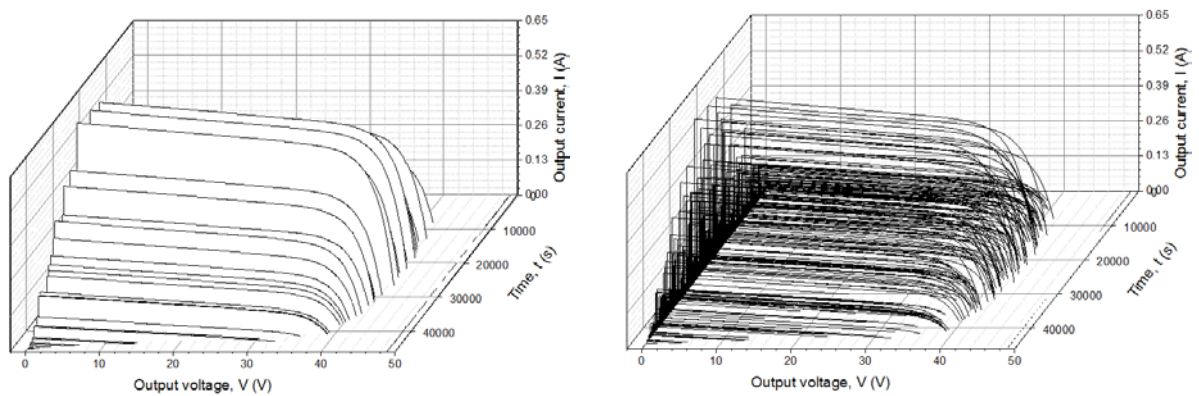


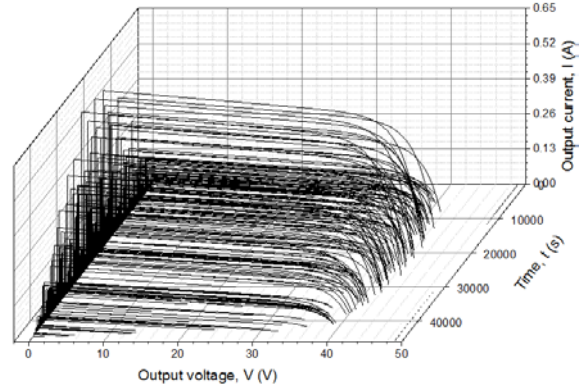
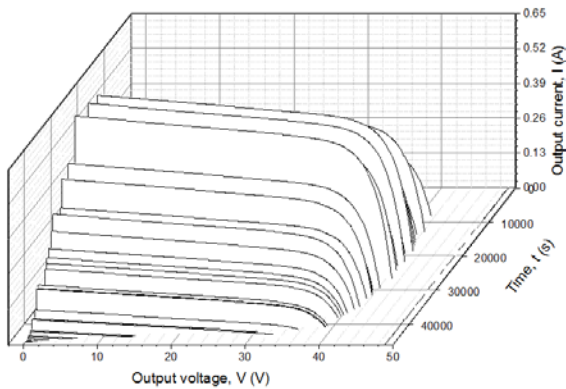
Figure 6b. Unmodified superimposed power-voltage curves for latitude, $\phi = 0.3476^\circ\text{N}$, slope, $\varphi=19.5^\circ$, month = January with 6:00am as a reference time



(i) Isometric view

(ii) Detailed view

Figure 7a. Unmodified superimposed current-voltage curves for latitude, $\phi = 0.3476^\circ\text{N}$, slope, $\varphi=19.5^\circ$, month = January with 6:00am as a reference time



(i) Isometric view

(ii) Detailed view

Figure 7b. Modified superimposed current-voltage curves for latitude, $\phi = 0.3476^\circ\text{N}$, slope, $\varphi=19.5^\circ$, month = January with 6:00am as a reference time

Cross examination of Figure 8 with respect to Figures 4 – 7, shows that the simulated unmodified simple condition produced pseudo; voltage and power above the exaggerated manufacturer’s specification but the simulated modified simple condition yielded a practical or true; voltage and

power, thus, it is imperative that the modified parameters (in Equations 11 – 16), should proceed the actual operating condition (AOC) computation rather than applying the unmodified condition as input data to the AOC computations, which contributed in falsifying the PVG simulated performance characteristics.

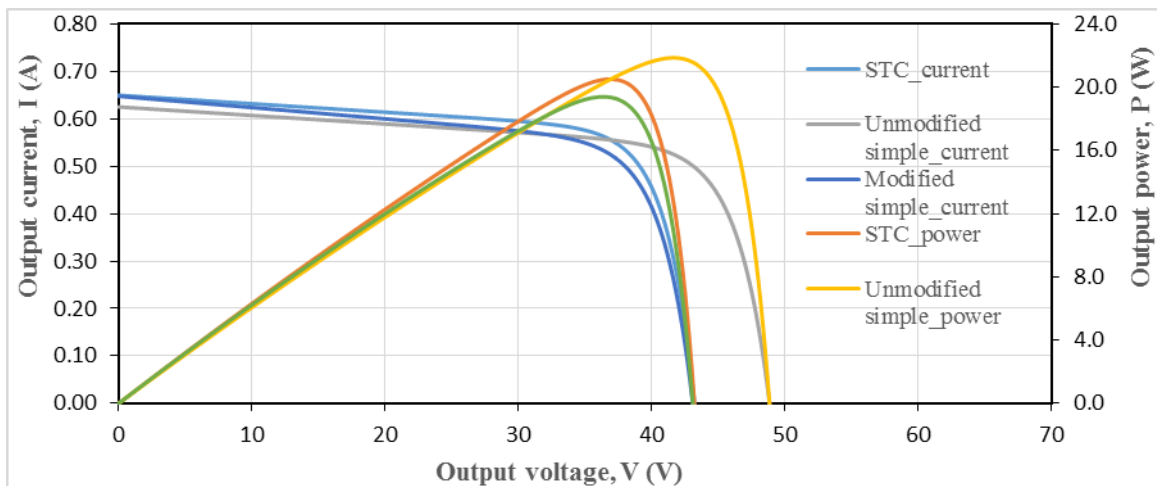


Figure 8. Composite plot of I_V and P_V for simple condition, latitude, $\phi = 0.3476^\circ\text{N}$, slope, $\varphi=19.5^\circ$, month = January with 6:00am as a reference time.

The insolation has a strong influence on the output current according to Wasfi [35], this is buttressed by the fact that the output current function in Figure 9 replicates the insolation function in Figure 2. In the same vein, the output power function in Figure 11 resembles the insolation function in Figure 2, thus, depicting that the output current and power is integrally dependent on the insolation as proposed by Abuella and Chowdhury [36]. However, Figure 10 does not maintain the functional trend in Figure 2, rather it mimics the PV-cell temperature function, which unequivocally supports that the voltage is specifically influenced by the PV-cell temperature whereas the insolation is glaringly responsible for flickers in the output voltage.

The response of the PV-cell temperature to the external stimuli (insolation, ambient temperature and wind speed) is dominated by the insolation, which implies that PV-cell temperature is more sensitive to insolation than the other external stimuli (ambient temperature and wind speed).

The voltages (open circuit, maximum power point and output) are susceptible to PV-cell temperature changes than the insolation [26, 37]. Drop in PV-cell temperature increases the voltages of PVG, which increases the efficiency of the PVG and vice-versa. The fluctuations in insolation induce instability in voltages, especially the output voltage.

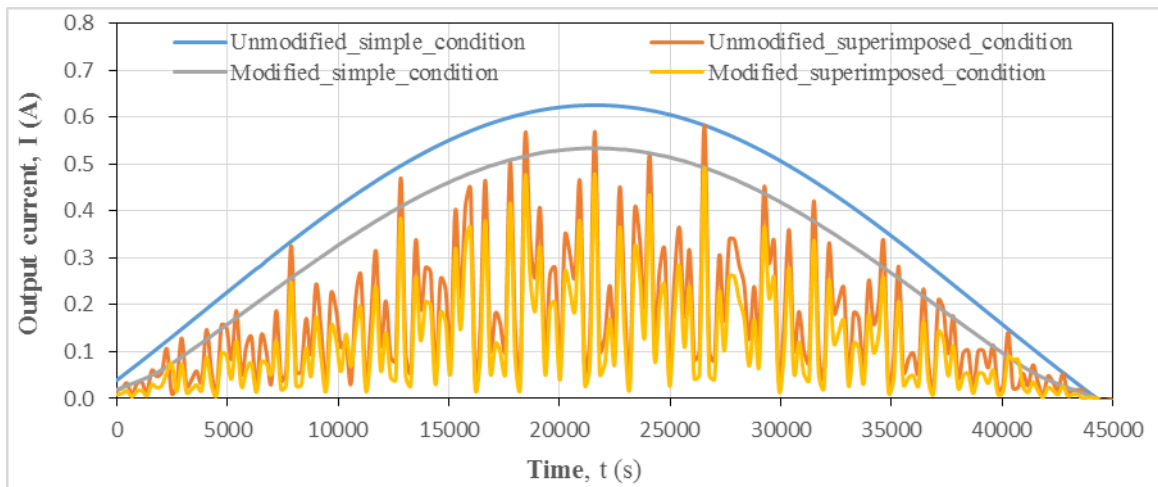


Figure 9. Hourly variation of maximum output current for latitude, $\phi = 0.3476^\circ\text{N}$, slope, $\varphi=19.5^\circ$, month = January with 6:00am as a reference time.

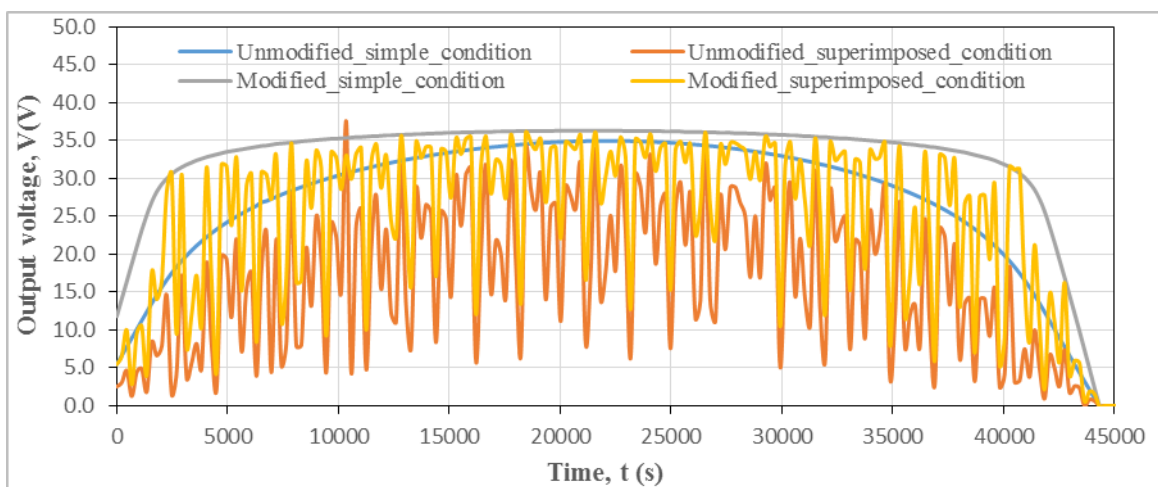


Figure 10. Hourly variation of maximum output voltage for latitude, $\phi = 0.3476^\circ\text{N}$, slope, $\varphi=19.5^\circ$,

month = January with 6:00am as a reference time.

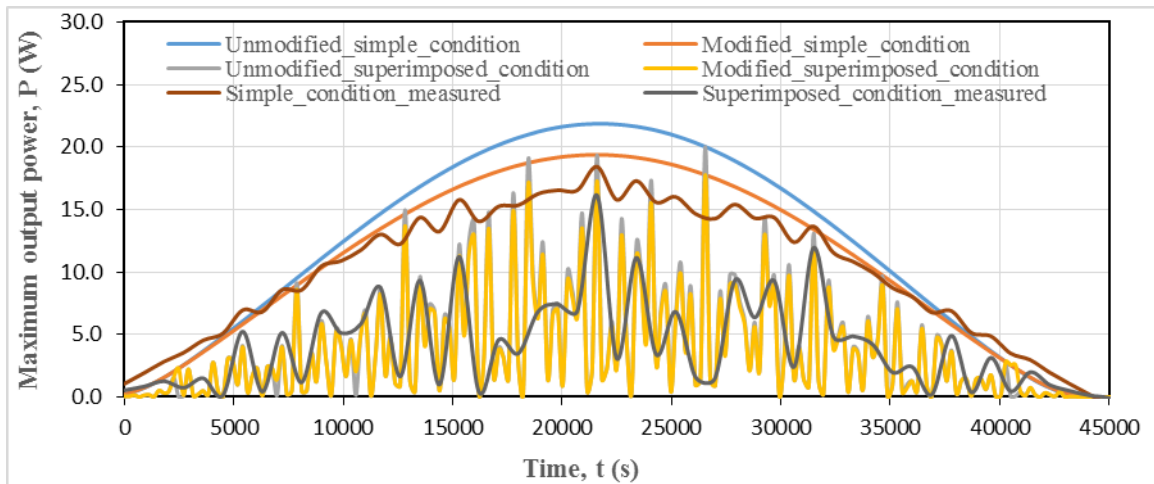


Figure 11. Hourly variation of maximum output power for latitude, $\phi = 0.3476$ °N, slope, $\varphi=19.5^\circ$, month = January with 6:00am as a reference time.

Reduction in power is pronounced at the sunrise, which is characterized with high concentration of moving clouds and similarly, during the sunset which witnesses high concentration of moving clouds. The clearness index at sunrise and sunset is forced lower by the concentration of the moving clouds resulting in a drastic reduction ($-\Delta P/P \rightarrow 1$) in the output power in Figure 12. Contrarily, the minimal reduction in power ($-\Delta P/P \rightarrow 0$) occurred at noon day indicating that the clearness index is at its peak value, thus, maximum power harvest occurred at 12:00pm, which is time the output power approaches the manufacture's rated power. Comparing the two conditions under study, it is obvious that reduction in power is immense and imminent under superimposed condition compared to simple condition.

Inevitably, there is likelihood of façade in the rating of the PVG by the manufacturers in order to attract good market value. Applying this rating to design of PVG plant may result in under performance of the plant. Thus, it is imperative that the PVG be subjected to field test in order to ascertain its true performance, which to achieve precision in the PVG plant design and operation. Based on the operation of the Cozy Mira PV, the practical rating in Figure 13 is less than the manufacturer's rating at any time. Equations 27 – 29 were used to develop a correction factor (as a rule of thumb), which suggests that for m-silicon semiconductor, the manufacturer's rating

should be scaled down by $\approx 4\%$ in order to minimize error in the design of PVG plants.

Lastly, Figure 13 describes the performance of the PVG, considering the tangents between the simulated and manufacturers' efficiencies represent the most efficient (or effective) period for harvesting power from the PVG, that is between 14400 s ($\equiv 10:00\text{am}$) and 28800 s ($\equiv 2:00\text{pm}$). 5.0

5.0 Conclusions

The dynamic analysis of performance of photovoltaic generators under moving cloud conditions has been successfully carried out; the façade in the specification of PVG by the manufacturers is as much as 4% scale up from the practical performance value. However, under-performance of large PV plants could be majorly attributed to the moving clouds, especially during the superimposed or strong cloud condition, which is usually marked with dark grey rainy clouds (nimbus) and partly due to apparent specification by the manufacturers. Thus, under-performance becomes a serious issue when large PV plants are designed on the basis of the manufacturer's rating. Consequently, the actual peak power will be defined below the designed value. However, the reduction in power becomes trifling during the simple or mild cloud conditions, because power is persistently being harvested during these conditions, which is compatible and permeable by the insolation. Thus, this work vehemently suggests that modules to be

applied in setting up large PV plants should be subjected to field tests or have its efficiency, scaled down by approximately 4% in order to establish the

actual capacity of the PV plant under the moving cloud conditions.

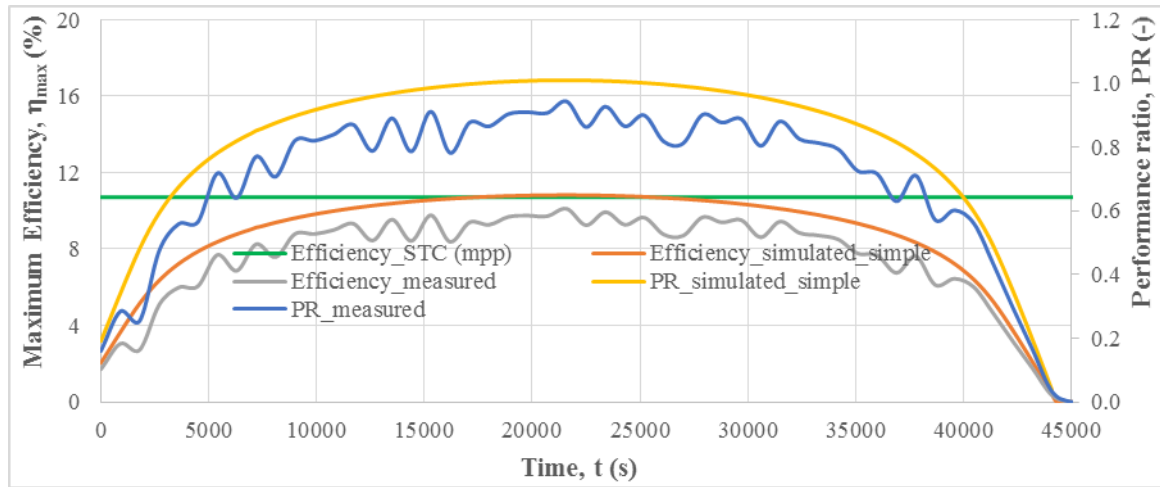


Figure 13. Rating of PVG at maximum output power for latitude, $\phi = 0.3476^\circ\text{N}$, slope, $\varphi = 19.5^\circ$, month = January with 6:00am as a reference time.

Acknowledgements

We appreciate the meteorological centers (NASA, ACCUWEATHER and HOMERENERGY) for availing data used in this work and KIU management for providing research facilities used in this work.

Competing interests

The authors declare that they have no competing interests.

Declaration of Funding

The authors wish to declare that there is no funding for this work.

References

1. Bonkaney, A., S. Madougou, and R. Adamou, *Impacts of cloud cover and dust on the performance of photovoltaic module in Niamey*. Journal of Renewable Energy, 2017. **2017**.
2. Mustafa, R.J., M.R. Gooma, and M. Al-Dhaifallah, *Environmental Impacts on the Performance of Solar Photovoltaic Systems*. Sustainability, 2020. **12**(2): p. 608.
3. Suri, M., et al. *Cloud cover impact on photovoltaic power production in South Africa*. in *Southern African Solar Energy Conference SASEC2014*. 2014.
4. Huld, T. *Estimating Solar Radiation and Photovoltaic System Performance, the PVGIS Approach*. in *AFRETEP 1ST Regional Workshop Kampala*. 2011.
5. Ye, J.-Y., et al., *Outdoor PV module performance under fluctuating irradiance conditions in tropical climates*. Energy Procedia, 2013. **33**: p. 238-247.
6. Woyte, A., R. Belmans, and J. Nijs, *Fluctuations in instantaneous clearness index: Analysis and statistics*. Solar Energy, 2007. **81**(2): p. 195-206.
7. Abdellatif, Y., et al., *Cloud Effect on Power Generation of Grid Connected Small PV Systems*. World Academy of Science, Eng, Tech IEEE, 2015. **9**(9).
8. Brecl, K., J. Kurnik, and M. Topič. *Evaluation of losses on energy yield due to self-shading of free standing PV systems*. in *24th European Photovoltaic Solar Energy Conference, Hamburg, Germany*. 2009.
9. Woyte, A., J. Nijs, and R. Belmans, *Partial shadowing of photovoltaic arrays with*

- different system configurations: literature review and field test results.* Solar Energy, 2003. **74**(3): p. 217-233.
10. Cirjaleanu, V., *Investigation of Cloud-Effects on Voltage Stability of Distribution Grids with Large Amount of Solar Photovoltaics.* 2017.
 11. Yan, R. and T.K. Saha, *Investigation of voltage stability for residential customers due to high photovoltaic penetrations.* IEEE transactions on power systems, 2012. **27**(2): p. 651-662.
 12. Nelson, J.A., *Effects of cloud-induced photovoltaic power transients on power system protection.* 2010.
 13. Cai, C. and D.C. Aliprantis, *Cumulus cloud shadow model for analysis of power systems with photovoltaics.* IEEE Transactions on Power Systems, 2013. **28**(4): p. 4496-4506.
 14. Marcos, J., et al., *Power output fluctuations in large scale PV plants: one year observations with one second resolution and a derived analytic model.* 2011. **19**(2): p. 218-227.
 15. Osman, Y.I.A., et al., *Experimental Study of the Cloud Influence on PV Grid Connected System.* 2018. **9**(1): p. 1-15.
 16. Bellini, A., et al. *Simplified model of a photovoltaic module.* in *2009 Applied Electronics.* 2009. IEEE.
 17. Nnamchi, S.N., et al., *Development of dynamic thermal input models for simulation of photovoltaic generators.* International Journal of Ambient Energy, 2018: p. 1-13.
 18. Esmeijer, K.B., *PV performance during low irradiance and rainy weather conditions.* 2014.
 19. Vijayalekshmy, S., G. Bindu, and S.R. Iyer. *Estimation of power losses in photovoltaic array configurations under moving cloud conditions.* in *2014 Fourth International Conference on Advances in Computing and Communications.* 2014. IEEE.
 20. Nguyen, D.D. and B. Lehman. *Modeling and simulation of solar PV arrays under changing illumination conditions.* in *2006 IEEE Workshops on Computers in Power Electronics.* 2006. IEEE.
 21. weather, A. *Kampala hourly weather – AccuWeather forecast for Wakiso Uganda.* 2018 [cited 2018 9th February]; Available from: www.accuweather.com/en/ug/Kampala.
 22. Energy, H. *Solar radiation, wind speed data for Kampala.* 2018 [cited 2018 9th February]; Available from: www.homerenergy.com/support/docs/3.11/publish.
 23. NASA. *Solar insolation.* 2018 [cited 2018 6th February]; Available from: www.power.larc.nasa.gov/solar/insolation.
 24. Klaus, J., I. Olindo, and H.M.S. Arno, *Basic semiconductor physics solar energy: fundamentals, technology, and systems.* 2014. 49-66.
 25. Cubas, J., S. Pindado, and F. Sorribes-Palmer, *Analytical calculation of photovoltaic systems maximum power point (MPP) based on the operation point.* Applied Sciences, 2017. **7**(9): p. 870.
 26. Nnamchi, S.N., et al., *Extrinsic modeling and simulation of helio-photovoltaic system: a case of single diode model.* International journal of green energy, 2019. **16**(6): p. 450-467.
 27. Boyd, M.T., et al., *Evaluation and validation of equivalent circuit photovoltaic solar cell performance models.* Journal of solar energy engineering, 2011. **133**(2).
 28. Ibrahim, H. and N. Anani, *Variations of PV module parameters with irradiance and temperature.* Energy Procedia, 2017. **134**: p. 276-285.
 29. Villalva, M.G., J.R. Gazoli, and E. Ruppert Filho, *Comprehensive approach to modeling and simulation of photovoltaic arrays.* IEEE Transactions on power electronics, 2009. **24**(5): p. 1198-1208.
 30. Bonkougou, D., Z. Koalaga, and D. Njomo, *Modelling and Simulation of photovoltaic module considering single-diode equivalent circuit model in MATLAB.* International Journal of Emerging Technology Advanced Engineering, 2013. **3**(3): p. 493-502.
 31. Oko, C., *Engineering Computational Methods; An Algorithm.* 2008, University of Port Harcourt, Press, Port Harcourt, Nigeria.
 32. Sathyanarayana, P., et al., *Effect of shading on the performance of solar PV panel.* Energy Power, 2015. **5**(1A): p. 1-4.
 33. Topic, M., K. Brecl, and J. Sites. *Performance Assessment of PV Modules-Relationship Between STC Rating and*

- Field Performance. in 2006 IEEE 4th World Conference on Photovoltaic Energy Conference. 2006. IEEE.*
34. Wasfi, M., *Solar energy and photovoltaic systems. 2011.*
35. Abuella, M. and B. Chowdhury. *Solar power forecasting using artificial neural networks. in 2015 North American Power Symposium (NAPS). 2015. IEEE.*
36. Nnamchi, S.N. and O.A. Nnamchi, *Perturbation of Diminutive Solar Irradiance and Extreme Semiconductor Temperature on the Output Current and Voltage: The Translation of Electrical Characteristics into Thermal Characteristics. Journal of Solar Energy Research, 2019. 4(2): p. 92-106.*